Wireless Power Transfer With Automatic Feedback Control of Load Resistance Transformation

Dukju Ahn, Seongmin Kim, Jungick Moon, and In-Kui Cho

***Abstract*—This paper proposes a wireless power transfer with automatic feedback control of load resistance transformation to maintain high efficiency over wide variations of coupling current and load current. The receiver (Rx) first determines the desired current level of transmitter (Tx) coil such that the receiver-side converter can transform the load resistance into optimum effective resistance, based on load current and Tx-to-Rx distance information. The determined Tx coil current data are sent to the transmitter, which then adjusts the Tx coil current accordingly. In this way, the effective resistance transformed by the receiver-side converter remains optimum under the variations of distance and load current. One of the advantages of the proposed automatic feedback control is faster response and simple hardware because it does not use operating point sweep and observation. The receiver-side switching converter also incorporates the ability to send data from receiver to transmitter by modulating the duty cycle of converter at data frequency, eliminating the need for separate RF communication hardware. This proposed communication does not require shunt current dissipation from dc output to ground, resulting in low loss. Experimental result demonstrates that the system maintains high efficiency under wide variations of coupling and load current.**

***Index Terms*—DC–DC converter, impedance matching, optimum load resistance, switching converter, wireless power.**

I. Introduction

WIRELESS power transfer is now widespread in a variety of applications ranging from milliwatts [1], [2], several watts [3], [4], to kilowatts [5], [6], [8]. One of the bottlenecks of wireless power technology is the ability to accommodate a wide range of distance and load variation. The alignment and distance separation between power transmitter (Tx) and receiver (Rx) change as the user moves the devices. In addition to the alignment, the current profile of typical rechargeable battery is decreased as charging status proceeds. Therefore, the wireless charging system should be robust under the varying load current.

It is well known that the efficiency usually degrades if the vertical separation or lateral misalignment becomes too large except for special cases such as overcoupled or bifurcation region. One of the solutions is to specially design the transmitter coil structure such as [5]–[7] so that the system is robust to misalignment. However, the coil structure proposed in [6] is not applicable for the scenario of vertical separation. Having two transmitters in [7] is not convenient. In other solutions, the inductance or capacitance value can be runtime adjusted if the distance or load is changed [9]–[11], at the expense of large array of discrete components. Frequency tracking is another method to compensate for the distance and load variations [21], [2]. Although these schemes successfully achieve output regulation, the limitation is that these are only applicable at short distance separation where frequency-splitting behavior is observed. The efficiency of [2] is severely degraded as the load resistance is changed. A number of multiresonator structures have been proposed to enhance the resonance and thereby extend the operating distance [22]–[25]. These multiresonators significantly enhance transmission distance and efficiency. However, the efficiency is still highly dependent on distance and load. Specifically, it has been pointed out that the efficiency of four-coil resonator is severely degraded at a very short distance [22]–[24].

Imura and Hori [12] demonstrated that the optimal load impedance, which produces maximum efficiency, is subject to change, depending on the air gap distance, and that selecting appropriate load impedance can avoid efficiency degradation without using inductor/capacitor tuning or frequency tracking. Garnica *et al*. [13] and Baker and Sarpeshkar [14] also discuss that there is an optimum resistance to which the load resistance needs to be matched in order to obtain maximum efficiency. The task is now to find the optimum load resistance and transform the actual load resistance into the optimum one. This point can be seen from Fig. 1. The effect of receiver coupled with transmitter is abstracted as a reflected resistance R_{refl}

$$R_{\mathrm{refl}} = k^2 \omega L_{\mathrm{Tx}} \frac{\omega L_{\mathrm{Rx}}}{R_{\mathrm{PRx}} + R_L}. \tag{1}$$

Since the power dissipation in the reflected resistance is equivalent to the actual power transferred to receiver, it is important to maintain high reflected resistance to increase efficiency. Unfortunately, the reflected resistance is dependent on coupling k and the load resistance R_L. In real application scenario, the coupling varies as the user alters the Tx-to-Rx alignment and the load resistance varies as the charging progresses or the device power consumption changes. Too small coupling k or too large load resistance R_L will lower the reflected resistance and degrade efficiency. In these cases, R_L needs to be transformed into a different effective resistance to compensate for the changes of coupling k or actual load R_L. Note that indefinitely high R_{refl} is also not desired because very high R_{refl} demands small R_L, and if R_L becomes too small and approaches R_{PRx}, then most of the power is dissipated in R_{PRx}, resulting in low efficiency.

Manuscript received September 10, 2015; revised November 11, 2015; accepted December 26, 2015. Date of publication December 29, 2015; date of current version June 24, 2016. This work was supported by the ICT R&D Program of MSIP/ETRI, Korea in 2015. Recommended for publication by Associate Editor Y. C. Liang.

D. Ahn is with Incheon National University, Incheon 22012, Korea (e-mail: adjj22@gmail.com).

S. Kim, J. Moon, and I.-K. Cho are with the Electronics and Telecommunications Research Institute, Daejeon 22012, Korea (e-mail: smkim97@etri.re.kr; jungick@etri.re.kr; cho303@etri.re.kr).

Color versions of one or more of the figures in this paper are available online at http://ieeexplore.ieee.org.

Digital Object Identifier 10.1109/TPEL.2015.2513060

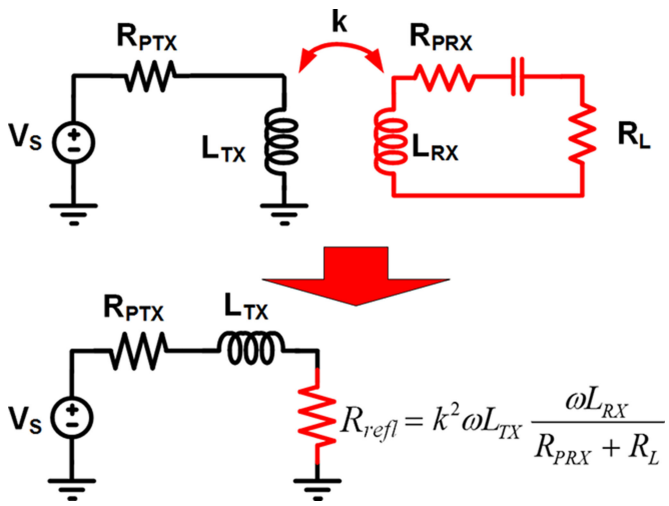

Fig. 1. Circuit model of basic wireless power transfer system. The effect of receiver is abstracted as a reflected resistance $R_{\rm refl}$. $R_{\rm refl}$ should be high to maintain high efficiency because the power dissipation in $R_{\rm refl}$ is equivalent to the power transferred to receiver. $R_{\rm PTx}$ is the sum of parasitic resistances of $L_{\rm Tx}$ and voltage source $V_{\rm s}$ $R_{\rm PRx}$ is the parasitic resistance of $L_{\rm Rx}$.

Therefore, there exists an optimal load resistance $R_{L,\rm opt}$ and a corresponding optimal $R_{\rm refl}$ as follows [13], [16]:

$$R_{L,\rm opt} = R_{\rm PRx}\sqrt{1+\frac{k^2\omega L_{\rm Tx}\omega L_{\rm Rx}}{R_{\rm PTx}R_{\rm PRx}}} \cong R_{\rm PRx}k\sqrt{\frac{\omega L_{\rm Tx}\omega L_{\rm Rx}}{R_{\rm PTx}R_{\rm PRx}}} \quad (2)$$

where the approximation holds if $k^2 * \omega L_{\rm Tx}/R_{\rm PTx} * \omega L_{\rm Rx}/R_{\rm PRx}$ is higher than unity, which is usually satisfied in weakly coupled system. For coupling k variation, the relationship (2) indicates that the variation of coupling alters the desired optimal load $R_{L,\rm opt}$, and the discrepancy between $R_{L,\rm opt}$ and R_L degrades efficiency. For load resistance variation, $R_{L,\rm opt}$ is not changed, and this discrepancy also degrades efficiency.

To address the challenge mentioned earlier, the idea of using a receiver-side switching converter has been proposed to transform the actual load resistance R_L into different effective load resistance, as well as output voltage regulation [15]–[18]. It is demonstrated that the receiver-side converter is able to transform the actual load resistance into effective load resistance, to increase the reflected resistance, and to improve the overall efficiency [15]. If the load resistance significantly deviates from the optimal load point or the coupling is reduced, the duty cycle of receiver-side switching converter is adjusted such that the reflected resistance and the overall efficiency are increased. The idea of using a switching converter to implement impedance transformation is advantageous over frequency tracking or inductor/capacitor (*L*/*C*) tuning because of larger distance separation, smaller *L*/*C* component size, and the ability to tune the parameters in continuous manner.

The amount of impedance transformation ratio needs to be runtime controlled to match the transformed resistance to the desired optimal value. This transformation ratio is not a fixed but variable value depending on distance and load condition. Several techniques have been developed to determine the optimal transformation ratio [16]–[18].

In [16], the input voltage to Tx inverter is adjusted to change the duty cycle of receiver-side dc–dc converter. Since the receiver-side converter forces the receiver output voltage to be constant, the optimal input voltage, which produces maximum efficiency, is equivalent to the input voltage, which results in the lowest input power. To find the optimal input voltage, the inverter input voltage is perturbed, the resultant input power is observed, and the input voltage is further perturbed based on the previous perturbation–observation cycle. The similar perturbation-and-observation method is demonstrated also in [17] and [18]. This algorithm successfully tracks the duty cycle of receiver-side converter, which yields the optimal load transformation and maximum overall efficiency.

Unfortunately, [15] lacks the ability to automatically adjust the duty cycle in response to load variation. Hence, the optimal duty cycle and Tx input voltage had to be manually adjusted. The perturbation-and-observation algorithm in [16]–[18] is able to track the optimal duty cycle automatically. However, the searching speed to find the optimum duty cycle tends to be slow. In [16, Fig. 14], one perturbation takes around 10 s. As an another example, in [18], one settling transient takes around 2–3 s under the variations of load and coupling. Another drawback is the complex and bulky control hardware such as FPGA, 2.4 GHz wireless communication module, RF coupler, and power sensor. Third problem is that its operating range needs to be restricted. Taking the study in [16] as an example, the duty cycle of 0.38 separates the system operating range into two regions, which have conflicting design requirements. Since the maximum efficiency point lies at the region of duty cycle higher than 0.38, the duty cycle was restricted accordingly such that the duty of 0.38 is the minimum allowed boundary. However, it is possible that the boundary duty value can be changed when the distance or load condition are changed. The work in [17] has a similar issue.

The work in [19] employs an active rectifier to maintain the current ratio between Tx coil and Rx coil to be constant. This feedback scheme is also effective for the reduced coupling and load variation scenario. To realize the feedback, the information on the rectifier switch-off cycle and the load output voltage has to be transmitted from receiver to transmitter via a separate wireless communication channel. It would be more compact and cost effective if the communication is via in-band load-shift keying (LSK) without having a separate wireless communication module.

In this paper, a method to determine the optimal duty cycle and the transformation ratio of the receiver-side converter is proposed. The distance separation and load current is sensed at receiver, which then sends a control value to transmitter such that the receiver converter can remain in optimal duty cycle. The scheme utilizes two analog feedback loops, one is internal to receiver and the other is from receiver to transmitter. It is different from perturbation and observation in that the duty cycle settles to the desired value by negative feedback from Rx to Tx without a sweeping process. The advantage is high efficiency over wide variation of distance and load current with fast response

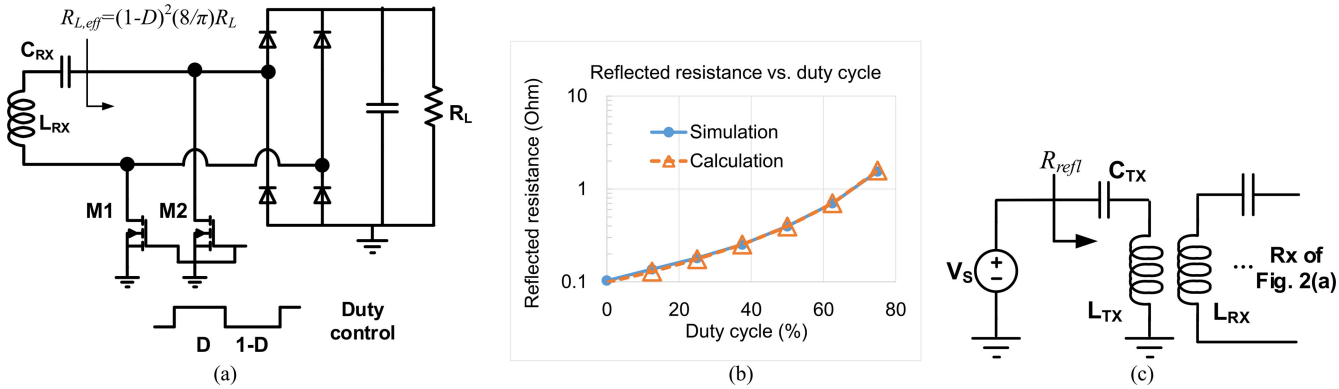

Fig. 2. (a) Boost-type converter attached at receiver resonator. (b) Simulated and calculated reflected resistance. It can be seen that the actual load resistance can be transformed into different value and, therefore, reflected resistance can be adjusted by changing the duty cycle of switching converter. $R_L = 9W$, $k = 0.074$, $L_{\mathrm{Tx}} = 3.96\mu\mathrm{H}$, and $L_{\mathrm{Rx}} = 9.33\mu\mathrm{H}$. (c) Simulation setup of (b).

and simple hardware. Section II describes the proposed technique, and Section III presents measurement result. Conclusion is drawn in Section IV.

II. Proposed Control Method

The aim of the proposed scheme is a fast, small-size, and low-cost feedback control of load resistance transformation of receiver-side converter. Utilizing feedback from receiver to transmitter is faster than perturbation-and-observation sweeping process. The proposed scheme does not need bulky and expensive hardware such as FPGA, microcontroller, or separate RF communication module.

The data flow of communication is only from receiver to transmitter—no communication is required from transmitter to receiver. The only feedback data that needs to be sent from Rx to Tx is the desired current level of Tx coil. This allows simpler communication scheme to be used. The conventional LSK communication consists of a shunt resistor and switch from rectifier output to ground in order to dissipate power at a data rate. This causes power loss at the communication resistor. To enable the low-loss communication from receiver to transmitter without separate RF module, the receiver-side switching converter equips with a new type of LSK back telemetry.

A. Control Strategy and Requirements

Fig. 2(a) illustrates the boost-type converter attached at the receiver resonator. When the two MOSFET switches are on, the resonant current is built up along $\mathrm{L_{Rx}}$–$\mathrm{C_{Rx}}$–M2–ground–M1. The switch is directly attached at the resonator before rectifier so that the current buildup path does not contain the rectifier, which has voltage drop loss. Another advantage is that separate dc inductor and output diode for a typical boost converter is not necessary. This is unlike the study in [15]–[17] where the switch comes after the rectifier. The rectifier converts R_L into $(8/\pi)R_L$, which is finally converted by boost switches into

$$R_{L,\mathrm{eff}} = (1-D)^2 \left(\frac{8}{\pi}\right) R_L \tag{3}$$

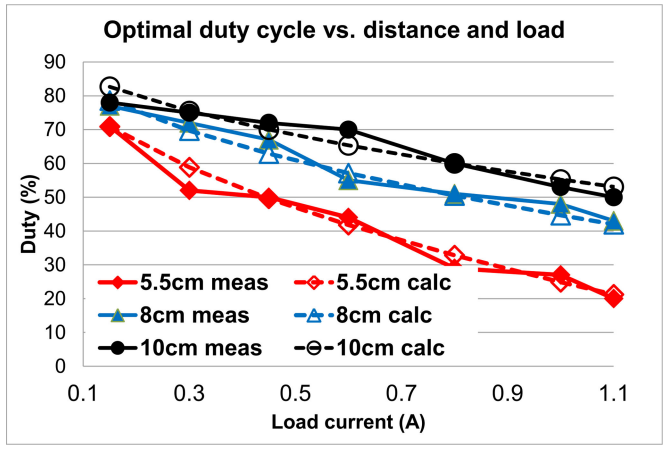

Fig. 3. Measured and calculated duty cycles for maximum efficiency under load current and coupling (distance) variations. It can be seen that higher duty cycle is required when the load current is small or the coupling coefficient is small.

where D is the duty cycle as described in [16]. Fig. 2(b) compares the simulated reflected resistance with calculated value using (3) and (1). It is seen that, by adjusting the duty cycle, the actual load can be transformed into a different value, which further modifies the reflected resistance. The simulation software is PSIM, which provides *RLC*, mutual inductance, and semiconductor switches. The simulated result of Fig. 2(b) matches the calculation very well because the diode and MOSFET are set to be lossless during simulation. The simulation setup is illustrated in Fig. 2(c). The reactance of L_{Tx} is cancelled by a resonating capacitor C_{Tx}, and the voltage source V_{s} supplies sinusoid voltage and current into the transmitter. The ratio between voltage and current of V_{s} is the reflected resistance.

Although smaller $R_{L,\mathrm{eff}}$ increases the reflected resistance, too small $R_{L,\mathrm{eff}}$ also reduces efficiency because the parasitic R_{PRx} becomes comparable with $R_{L,\mathrm{eff}}$. This is the reason why infinitely small $R_{L,\mathrm{eff}}$ is not desired, and there is an optimal value described as in (2). The optimal duty cycle is determined by coupling coefficient and load resistance. Fig. 3 illustrates the duty cycle for maximum efficiency under various load currents

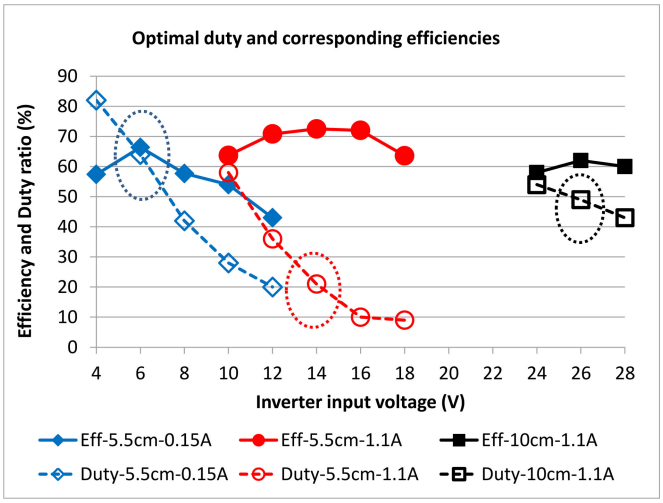

Fig. 4. Inverter input voltage and corresponding duty cycle and efficiency. Changing the inverter input voltage is a method of adjusting the receiver duty cycle. It can also be seen that the efficiency is maximized at a certain duty cycle. The inverter input needs to be high when coupling is low or load current is high. In this measurement, input voltage is directly fed from dc supply equipment. In practice, a dc–dc converter could be used to control the input voltage.

and distances. The measurement curve in Fig. 3 is obtained by manually sweeping the Tx inverter input and recording the corresponding duty cycle and efficiency. The calculation in Fig. 3 is done using (2) and (3). It can be seen that lower load current (i.e., larger load resistance) and longer distance (i.e., small coupling) demand higher duty cycle. This relationship can be explained by (2) and (3). The wireless power system is typically designed at its full load condition, which implies that nominal load resistance is typically small. However, when the load current becomes small (i.e., large load resistance), this large resistance needs to be reduced back to the nominal small resistance. Therefore, according to (3), high duty cycle is required. For small coupling condition, (2) describes that the optimal load resistance should be small, which means higher duty cycle is required.

The duty cycle is adjusted by changing the Tx coil current because receiver-side converter is regulated at a fixed dc output voltage. Fig. 4 illustrates the measured duty cycle and corresponding efficiency versus Tx input voltage, which is an indicator of Tx coil current. It can be seen that the Tx inverter input voltage needs to be high when the coupling is low. This can be explained as follows. When the coupling coefficient k is reduced, say half, the optimal load resistance $R_{L,\mathrm{opt}}$ also needs to be reduced by half. However, the power dissipation at reflected resistance

$$|I_{\mathrm{Tx}}|^2 R_{\mathrm{refl}} = |I_{\mathrm{Tx}}|^2 k^2 \omega L_{\mathrm{Tx}} \left(\frac{\omega L_{\mathrm{Rx}}}{R_{L,\mathrm{opt}}}\right) = \text{constant} \tag{4}$$

needs to be constant because the receiver output power is regulated to be constant, where I_{Tx} is the Tx coil current. Therefore, $|I_{\mathrm{Tx}}|^2$ needs to be increased to maintain constant output power at $R_{L,\mathrm{opt}}$. The fact that lower coupling demands higher Tx coil current can also be explained in the following way. Suppose that the Tx coil current I_{Tx} is fixed when the coupling coefficient k is reduced by half. Since the power consumption at reflected resistance

$$|I_{\mathrm{Tx}}|^2 R_{\mathrm{refl}} = |I_{\mathrm{Tx}}|^2 k^2 \omega L_{\mathrm{Tx}} \left(\frac{\omega L_{\mathrm{Rx}}}{R_{\mathrm{eff}}}\right) = \text{constant} \tag{5}$$

needs to be constant, $R_{L,\mathrm{eff}}$ is regulated to be reduced by 1/4. However, according to (2), $R_{L,\mathrm{opt}}$ needs to be reduced only by half if coupling is reduced by half. Therefore, the transformed $R_{L,\mathrm{eff}}$ value becomes different from the desired $R_{L,\mathrm{opt}}$ value, if the Tx coil current is not increased.

When the load current is reduced, it can be seen that the Tx coil current and inverter input needs to be reduced in Fig. 4. This is because $R_{L,\mathrm{opt}}$ is constant regardless of the load current, but the power dissipation $|I_{\mathrm{Tx}}|^2 * k^2 i\omega L_{\mathrm{Tx}}(\omega L_{\mathrm{Rx}}/R_{L,\mathrm{opt}})$ should be reduced.

Based on the aforementioned discussions, it can be summarized that the Tx coil current should be adjusted in order to adjust the receiver duty cycle. Table I summarizes the relationships discussed earlier.

TABLE I
CONTROL PARAMETER RELATIONSHIPS

	Distance Increased (Coupling Reduced)	Load Current Reduced (Load Resistance Increased)
Tx coil current	Increase	Reduce
Rx converter duty cycle	Increase	Increase
$R_{L,\mathrm{opt}}$	Reduced	Constant

B. Proposed Control Method

Fig. 5 illustrates the conceptual diagram of the proposed control method to implement the control strategy discussed earlier. The receiver senses the load current and coupling coefficient and then determines the required Tx coil current level, which is proportional to I_{sen}-$\mathrm{EA}_{\mathrm{out}}$. Here, the coupling coefficient is indirectly sensed by the duty cycle of Rx converter (or the voltage level of $\mathrm{EA}_{\mathrm{out}}$) because the Rx output is regulated at a constant dc voltage by the Rx-internal feedback loop. In other words, for example, the duty cycle of Rx converter is high if the coupling coefficient is reduced. Higher duty cycle implies lower coupling coefficient. The transmitter adjusts its Tx coil current amplitude based on the I_{sen}-$\mathrm{EA}_{\mathrm{out}}$ sent from receiver. In response to the change of Tx coil current, the duty cycle of the receiver-side switching converter is automatically adjusted by the feedback loop embedded in receiver.

When the load current is reduced, I_{sen} is lowered proportionally. I_{sen}-$\mathrm{EA}_{\mathrm{out}}$ is reduced accordingly, and this value is sent to the transmitter. As a result, the Tx coil current is reduced, resulting in higher duty cycle and smaller transformed resistance.

When the coupling coefficient is reduced, $\mathrm{EA}_{\mathrm{out}}$ is immediately reduced to produce larger duty cycle. At the same time, I_{sen}-$\mathrm{EA}_{\mathrm{out}}$ is increased to slowly increase the Tx coil current

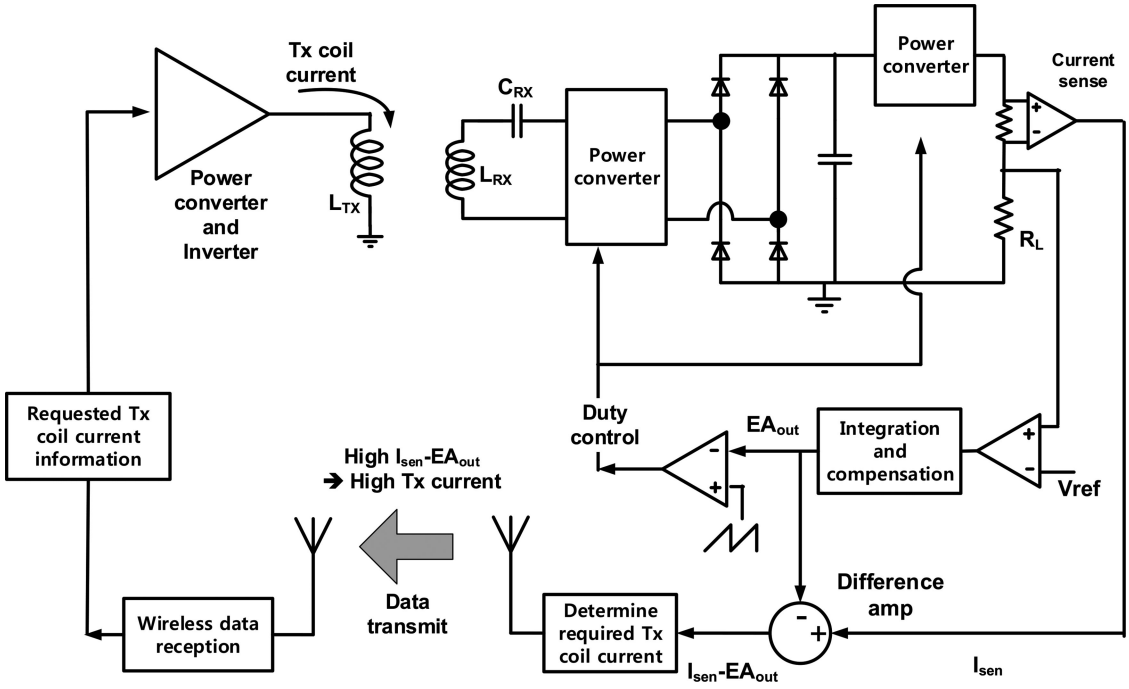

Fig. 5. Conceptual diagram of the proposed control method. The receiver determines the desired Tx coil current which is proportional to $I_{\rm sen}$-$\rm EA_{out}$. This is sent to the transmitter in order to adjust the Tx coil current. The receiver-side converter duty cycle is changed in response to the adjusted Tx coil current by the receiver internal feedback. In this way, the receiver duty cycle is settled to the optimum duty cycle, which transforms R_L into $R_{L,\rm opt}$.

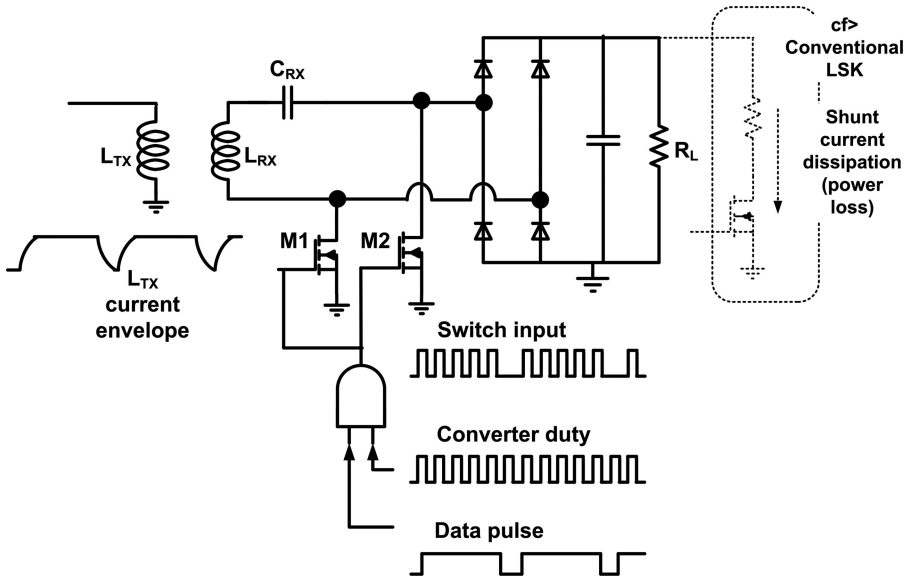

Fig. 6. Proposed LSK back telemetry, which transmits data from receiver to transmitter. The conventional LSK is also illustrated as a comparison by dotted lines. Unlike the conventional LSK, the proposed LSK does not dissipate power from shunt resistance, resulting in low loss. The switching converter M1–M2 stops at the data pulse rate. This causes current pulse at Tx coil.

amplitude. Since the Tx coil current is increased, the reduced $\rm EA_{out}$ is slightly recovered and the amount of increment of duty cycle is somewhat reduced. In other words, the duty cycle increases as the coupling coefficient is reduced, but the amount of increment of duty cycle is rather low due to the Tx coil current increment. The rationale of this control strategy is explained in (4), (5), and corresponding discussions.

Although Fig. 5 illustrates two power converters before and after the rectifier, the number and the placement of power converter can be freely chosen based on application situation. For example, only one power converter either before or after the rectifier can also implement the proposed control concept. Similarly, the data communication can be either a separate wireless channel or an in-band LSK.

C. Proposed LSK Communication with Switching Converter

Fig. 6 illustrates the proposed back telemetry scheme, which transmits data from receiver to transmitter. Fig. 6 also compares

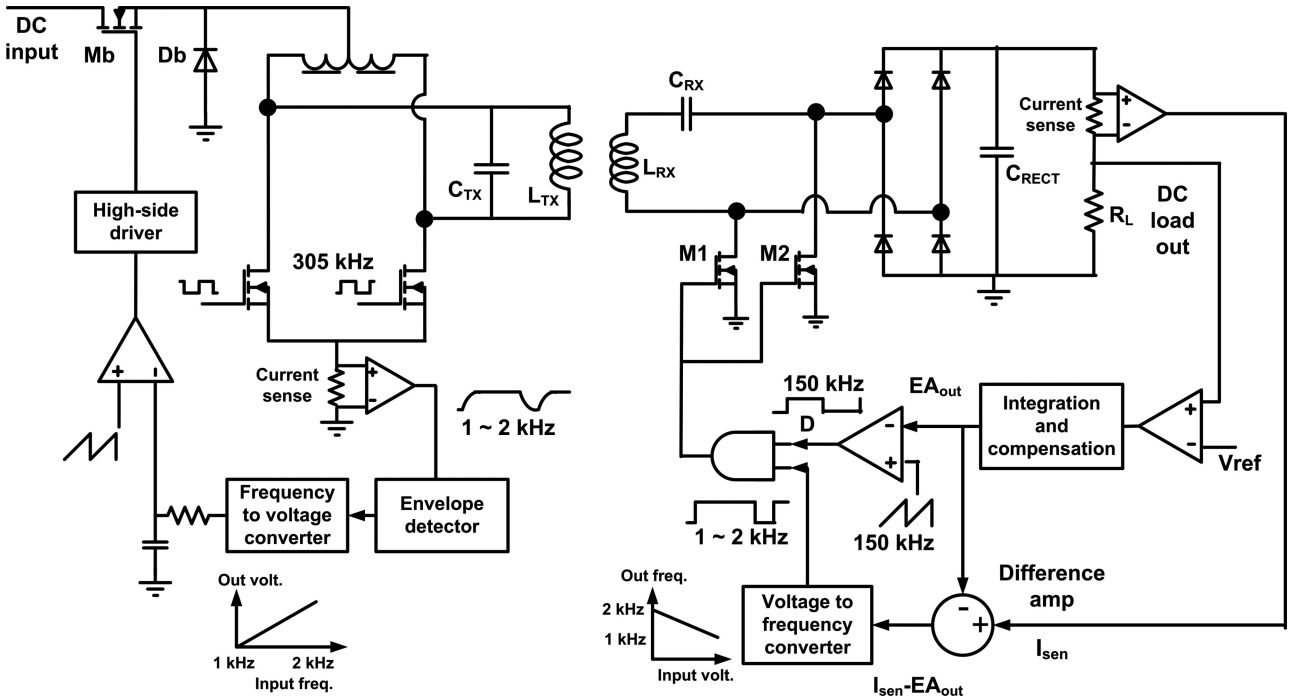

Fig. 7. Circuit implementation of the proposed control method of Figs. 5–6. The M1–M2 is the receiver-side switching converter whose duty is controlled by the feedback loop. The feedback loop finds the optimum duty of M1–M2 such that R_{L} is transformed to $R_{\mathrm{L,opt}}$, as well as performs dc-load voltage regulation. M1–M2 also performs LSK back telemetry communication.

the conventional LSK scheme with proposed one. Unlike the conventional LSK back telemetry scheme [20], the proposed LSK does not have the shunt current dissipation path from dc output through resistor to ground. This has the advantage of avoiding power loss during the communication switch-on duration. Instead of using the traditional shunt current path and resistor, the proposed scheme slowly modulates the converter (M1 and M2) duty cycle at a data frequency. This induces the variation of Tx coil current envelope at a data frequency, and data are recovered by Tx demodulator.

D. System Implementation

Fig. 7 illustrates a specific circuit implementation of the proposed method of Figs. 5 and 6. I_{sen}-$\mathrm{EA}_{\mathrm{out}}$ voltage level is converted to frequency quantity using LTC6992 voltage-controlled oscillator. This modulates the gate input to M1 and M2, and this frequency is detected by an envelope detector within the transmitter. The data communication does not need digital modulation because it is sufficient to send only a single voltage quantity I_{sen}-$\mathrm{EA}_{\mathrm{out}}$. Instead of digital encoding, high I_{sen}-$\mathrm{EA}_{\mathrm{out}}$ voltage is mapped to low-frequency pulse, which is directly recovered to a low voltage value by a frequency-to-voltage converter.

The recovered voltage value at the frequency-to-voltage converter determines the PWM duty ratio of a transmitter buck converter consisting of Mb–Db. The current in L_{Tx} is directly controlled by the duty cycle of Mb.

III. Experimental Result

Fig. 8 is the measurement setup. The Tx coil diameter and Rx coil diameter is 12.5 and 11.5 cm, respectively. The distance

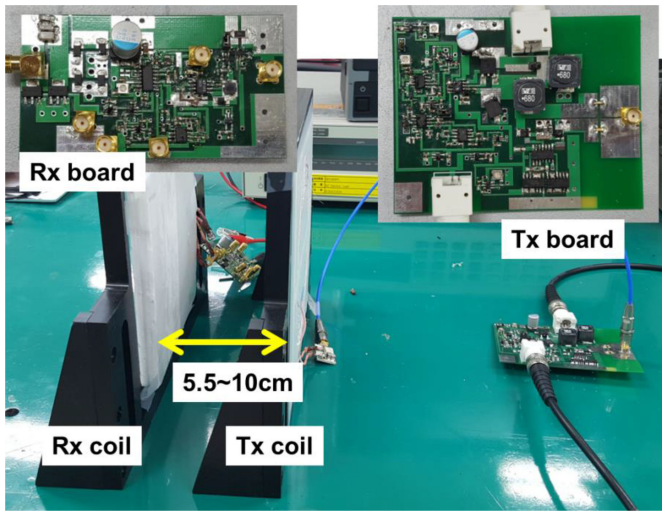

Fig. 8. Measurement setup and fabricated Tx and Rx boards.

between Tx coil and Rx coil is varied between 5.5 and 10 cm. The inverter frequency is 305 kHz, while the receiver-side converter frequency is 150 kHz. The Tx coil is single-layer, five-turn litz wire, and the Rx coil is a double-layer, eight-turn litz wire. The bench-top dc power supply provides the supply voltage to Tx inverter, and the electronic load draws dc current from Rx board output, which is regulated at 9.15 V. The total efficiency is measured by the dc output power of electronic load divided by the dc supply power of Tx inverter. Table II summarizes the system parameters.

Fig. 9 shows the measured waveform when the Tx-to-Rx distance is fixed and the load current is varied. Fig. 9(a) and (b)

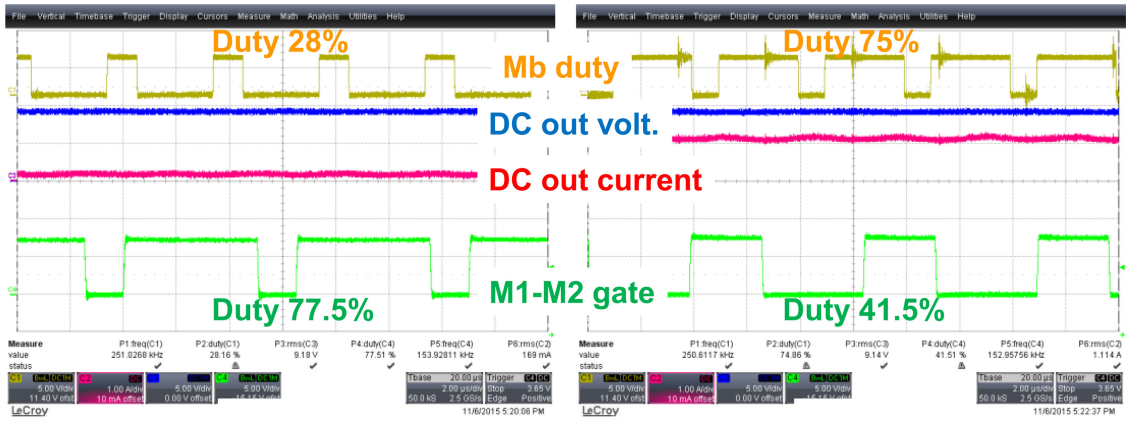

Fig. 9. Measured waveform when the Tx-to-Rx distance is fixed to 8 cm and the load current is varied. (a) Load current of 0.15 A. (b) Load current of 1.1 A. For lower load current, the receiver-side duty cycle is increased and the Tx coil current is decreased.

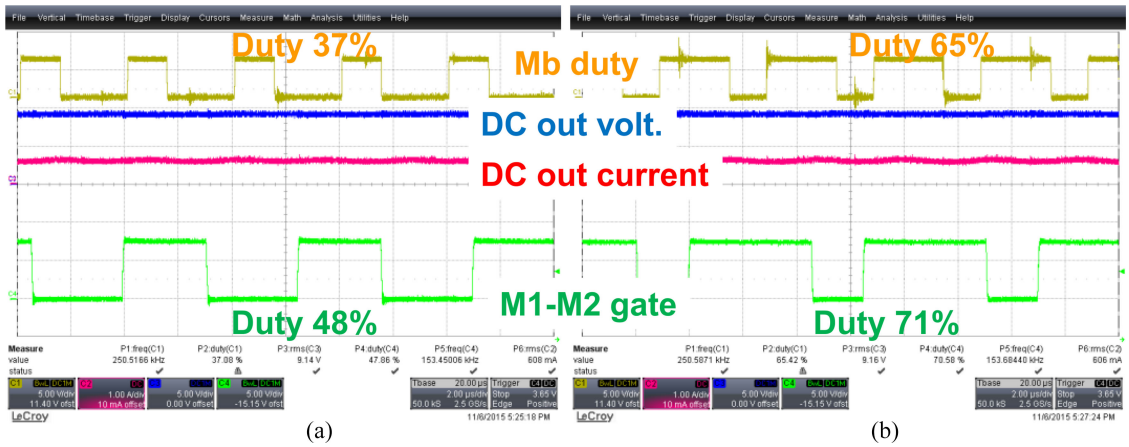

Fig. 10. Measured waveform when the load current is fixed to 0.6 A and the distance is varied. (a) Tx-to-Rx distance is 5.5 cm. (b) Tx-to-Rx distance is 10 cm. For larger distance separation, the receiver-side duty is increased and the Tx coil current is also increased.

TABLE II
SYSTEM PARAMETERS

Parameter	Value
L_{Tx}	3.96 μH
R_{PTx}	0.035 Ω
L_{Rx}	9.33 μH
R_{PRx}	0.06 Ω
C_{Tx}	71 nF
C_{Rx}	30 nF
C_{RECT}	680 μF
Load voltage	9.15 V
Load current	0.15–1.1 A
Inverter frequency	305 kHz
Inverter dc input	26 V
Tx coil diameter	12.5 cm
Rx coil diameter	11.5 cm
Tx-to-Rx distance	5.5–10 cm

shows the load current of 0.15 and 1.1 A, respectively. It can be seen that when the load current is small as in Fig. 9(a), the Tx input current is lowered by lowering the Tx buck converter duty cycle Mb. At the same time, the duty cycle of the receiver-side converter M1–M2 is increased to transform the large load resistance into a smaller value as explained in Section III-A.

Fig. 10 is the measured waveform when the load current is 0.6 A. Fig. 10(a) and (b) shows the Tx-to-Rx distance of 5.5 and 10 cm, respectively. When the distance is long, the Tx input current is increased by higher Mb duty, and the duty cycle of the receiver-side converter is increased, as explained in Section III-A.

Fig. 11 shows the measured waveform of the Rx dc output, the Tx demodulator output, and the receiver-side converter duty input. Note that the timescale is longer compared to Figs. 9 and 10 to visualize the LSK communication situation. The M1–M2 gate input is set to zero at a data rate. This variation in the duty cycle of the receiver converter is detected and demodulated by Tx-side envelope detector. The advantage of this communication is that it does not dissipate the power through a shunt resistor unlike the conventional LSK scheme. The communication burden of the proposed feedback control is simple—it is sufficient to send a voltage value (I_{sen}-$\mathrm{EA}_{\mathrm{out}}$) from the receiver to transmitter. Therefore, modulation/demodulation can easily be implemented by mapping the I_{sen}-$\mathrm{EA}_{\mathrm{out}}$ value to the

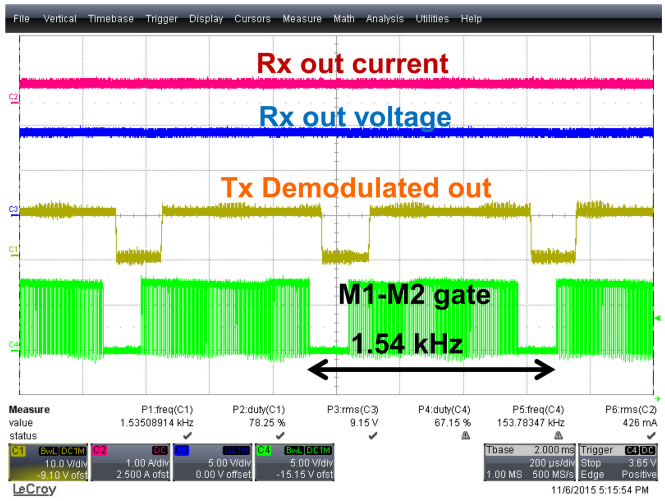

Fig. 11. LSK communication waveforms. The Rx-side converter M1–M2 is off at a rate of data pulse (1.48 kHz in this setup). This is demodulated at Tx. Low-loss LSK is realized by the activation/deactivation of Rx-side switching converter without the shunt power dissipation of traditional LSK. Output current is 450 mA.

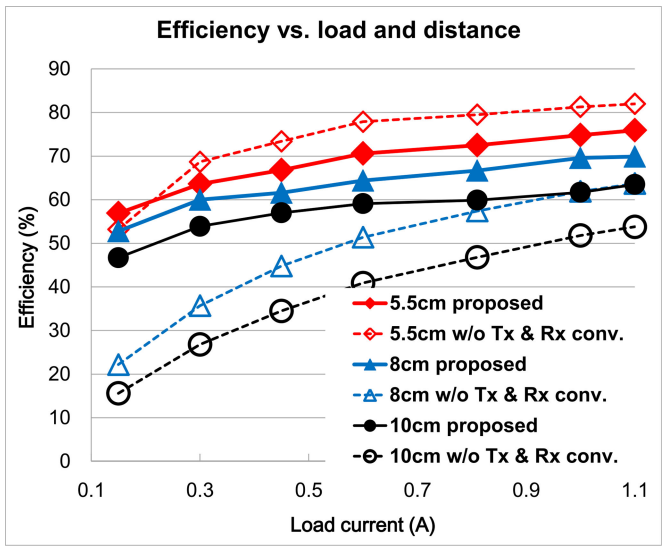

Fig. 12. Measured efficiency under the variations of coupling and load current. The Rx-side converter for optimum load resistance transformation is effective to increase the efficiency at small load current or longer distance. The "w/o conv." traces are measured by disabling Mb–Db and M1–M2 shown in Fig. 7. In practice, conventional wireless power systems have a dc–dc converter at transmitter inverter. Therefore, the efficiency of conventional systems would be reduced in actual deployment scenario.

communication frequency, and complex digital hardware is not necessary.

Fig. 12 shows the measured efficiency under the variations of coupling and load current. Without the receiver-side converter, the efficiency is significantly degraded when the load current is reduced or the distance is increased. This severe efficiency degradation is avoided by the load resistance transformation of the receiver-side converter. For a very strong Tx–Rx coupling as in 5.5 cm distance gap, the system without Tx/Rx switching converter might perform better. In practice, conventional wireless power systems have a dc–dc converter at transmitter

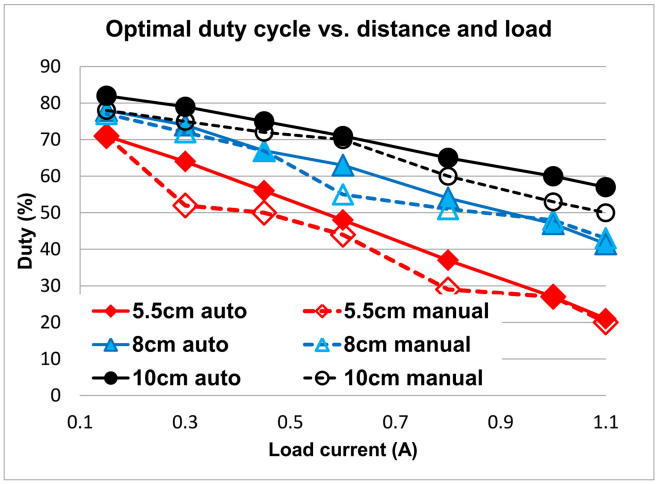

(a)

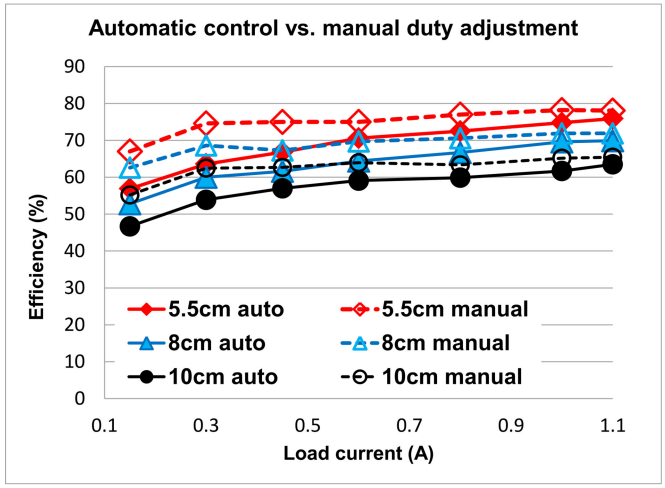

(b)

Fig. 13. (Solid line) Measured duty cycle and efficiency settled by automatic feedback control. (Dotted line) Measured optimum duty cycle and efficiency by manual adjustment of Tx input voltage. (a) It can be seen that the automatic feedback loop indeed tracks the optimum duty cycle. (b) Measured efficiency. The automatic feedback control nearly achieves maximum efficiency found by manual duty adjustment. The efficiency difference happens at smaller load currents due to the low efficiency of Tx dc–dc converter consisting of Mb–Db in Fig. 7.

inverter, which will reduce the efficiency of conventional system in actual deployment scenario. Moreover, its efficiency is severely degraded if the distance becomes longer or the load current is reduced. Therefore, the basic wireless power without any load transformation is hard to accommodate wide variation of distance and load. On the other hand, the proposed scheme is very robust to distance and load variation.

Moreover, the ability to receive the required amount of power is greatly increased with the proposed system. The "10 cm w/o Tx & Rx conv." setup can only receive up to 6 V output voltage, whereas the "10 cm proposed" setup can successfully receive 9.15 V. The proposed scheme receives higher power without increasing the coil current I_{Tx}, because the proposed scheme increases reflected resistance R_{refl} and the power delivered to the receiver is equivalent to $I_{\mathrm{Tx}}^2 R_{\mathrm{refl}}$.

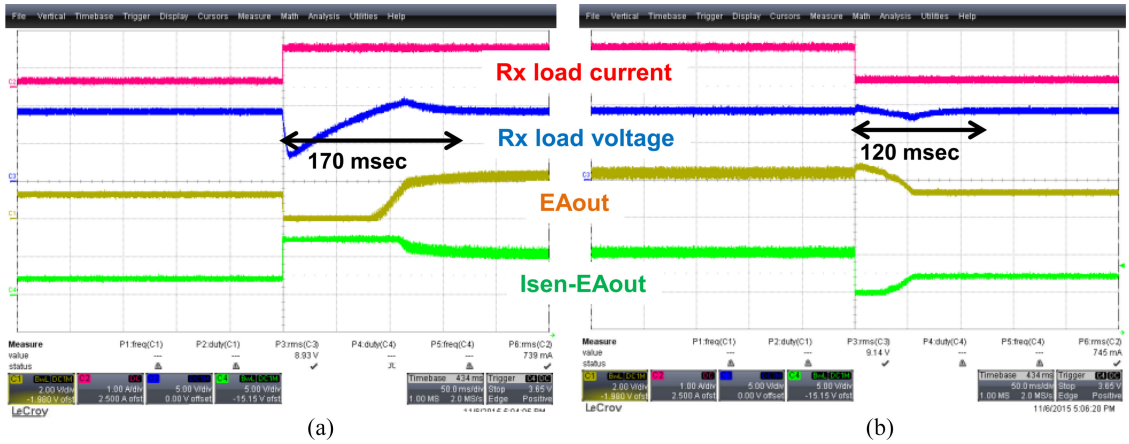

Fig. 14. Transient waveforms when the load current is changed. The output settles within 170 ms. This response is faster than the perturbation-and-observation method.

TABLE III
PERFORMANCE COMPARISON

	Tx Coil Size (cm)	Rx Coil Size (cm)	Distance (cm)	Normalized Distance	Coupling Coefficient	Power Setup	Efficiency (%)	Settling Time
This paper	12.5	11.5	5.5	0.46	$k = 0.137$	10 W	76	170 ms
			5.5	0.46	$k = 0.137$	2.7 W	64	
			10	0.83	$k = 0.048$	10 W	63.5	
[16]	2.7	2.7	n/a	n/a	$k = 0.1$	2.5 W	35	>20 s
					$k = 0.44$	4.5 W	65	
[17]	27	27	10	0.37	n/a	25 W	88	n/a
			25	0.93		25 W	73	
			25	0.93		100 W	79	
[18]	32	32	10	0.31	$k = 0.075$	Input 40 W	78	A few seconds
			7	0.22	$k = 0.137$		73	

For the curves without the Tx/Rx converter, the output voltage is not automatically regulated. Instead, the output voltage is manually set to be 9.15 V, which is the same voltage as switching converter case. To do this, the input voltage of inverter is manually adjusted to produce 9.15 V output by dialing the benchtop power supply knob. One exception is for the "10 cm w/o Rx conv." curve—the achievable output voltage was at most 6 V even if the inverter input voltage is increased to maximum limit. For the curves with the "proposed" labels, the output voltage is automatically regulated to 9.15 V. Both the proposed scheme and the "w/o Tx & Rx conv." setup can maintain constant Rx load voltage by increasing the Tx inverter output power when the efficiency is degraded. However, the advantage of the proposed scheme is that the efficiency degradation is milder compared to "w/o conv." system, resulting in lower power demand to maintain the same load voltage.

Fig. 13(a) compares the proposed automatically controlled duty cycle with the manually found maximum-efficiency duty cycle. It can be seen that the proposed control loop is able to track the optimum duty cycle of the receiver and, therefore, maximum efficiency load resistance point. Fig. 13(b) compares the efficiency difference between automatic feedback control and manual optimal duty sweeping. Although the automatic feedback nearly accomplishes the maximum efficiency found by manual adjustment, there exists slight efficiency difference between the two control methods. The efficiency of automatic feedback is lower because it uses an additional dc–dc converter at the input of Tx inverter (Mb–Db in Fig. 7), whereas the input voltage of manually adjusted system is manually controlled by dc supply equipment. The efficiency difference becomes larger at smaller load currents because the efficiency of the Tx dc–dc converter is low at low output power. In fact, the measured efficiencies of the Tx dc–dc converter are 96%, 92%, and 86% for Rx load current of 1.1, 0.6, and 0.15 A, respectively. Nevertheless, the efficiency improvement due to the proposed method is much higher than the loss due to Tx dc–dc converter, which leads to overall efficiency improvement compared to no converter traces as in Fig. 12.

Fig. 14 shows the transient waveform when the load current is changed. The output voltage settles within 170 ms, which is much faster than the perturbation-and-observation systems such as [16]–[18] because the proposed scheme does not involve operation point alteration and observation. While the internal feedback loop of receiver is much faster, the 170 ms delay is mainly due to the slow feedback from receiver to transmitter. Specifically, the *RC* low-pass filter at the output of the frequency-to-voltage converter in Fig. 7 sets the loop speed.

Table III compares this paper with perturbation-and-observation-based systems. The efficiency is comparable with other systems when the distance and output power level are similar. The settling time of this paper is the fastest.

IV. Conclusion

This paper proposes a wireless power transfer system with automatic feedback control of load resistance transformation in order to achieve high efficiency over the wide variations of coupling coefficient and load current. When the coupling coefficient or load resistance is varied, the present actual load resistance becomes different from an optimum load resistance, which produces maximum efficiency. While the receiver-side converters can, in theory, transform the actual load resistance into the optimum resistance, it has been hard to determine the appropriate transformation ratio such that the transformed resistance matches to the optimum resistance.

This paper solves the aforementioned problem by feedback loop, which senses the load current and the coupling coefficient. Here, the variation of coupling coefficient is indirectly sensed by the duty cycle of Rx-side converter. The coupling coefficient and the load current together determine the desired Tx coil current level, which is sent to transmitter via low-loss LSK communication. The Tx coil current is adjusted according to the received data via LSK, then the receiver duty cycle is finally adjusted in response to Tx coil current variation. Adjusting the receiver duty cycle is equivalent to adjusting the load transformation ratio.

The system does not require any separate wireless communication module, or operating point sweeping using microcontrollers or FPGA. Instead, a feedback is performed by simple and low-cost hardware with fast speed. Measurement results show that the feedback loop indeed transforms the original load resistance very close to the optimum load resistance. As a result, significant efficiency improvement is achieved over wide variations of coupling and load resistance.

References

[1] M. Zargham and P. Gulak, "Maximum achievable efficiency in near-field coupled power-transfer systems," *IEEE Trans. Biomed. Ckt. Syst.*, vol. 6, no. 3, pp. 228–245, Jun. 2012.

[2] D. Ahn and S. Hong, "Wireless power transmission with self-regulated output voltage for biomedical implant," *IEEE Trans. Ind. Electron.*, vol. 61, no. 5, pp. 2225–2235, May 2014.

[3] P. Riehl, A. Satyamoorthy, H. Akram, Y.-C. Yen, J.-C. Yang, B. Juan, C.-M. Lee, F.-C. Lin, V. Muratov, W. Plumb, and P. Tustin, "Wireless power systems for mobile devices supporting inductive and resonant operating modes," *IEEE Trans. Microw. Theory Tech.*, vol. 63. no. 3, pp. 780–790, Mar. 2015.

[4] K.-G. Moh, F. Neri, S. Moon, P. Yeon, J. Yu, Y. Cheon, Y.-S. Roh, M. Ko, and B.-H. Park, "A fully integrated 6W wireless power receiver operating at 6.78 MHz with magnetic resonance coupling," in *Proc. ISSCC*, 2015, pp. 230–232.

[5] J. Huh, S. Lee, W. Lee, G. Cho, and C. Rim, "Narrow-width inductive power transfer system for online electrical vehicles," *IEEE Trans. Power Electron.*, vol. 26, no. 12, pp. 3666–3679, Dec. 2011.

[6] C. Park, S. Lee, S. Jeong, G.-H. Cho, and C. Rim, "Uniform power I-type inductive power transfer system with DQ-power supply rails for on-line electric vehicles," *IEEE Trans. Power Electron.*, vol. 30, no. 11, pp. 6446–6455, Nov. 2015.

[7] S. Cheon, Y.-H. Kim, S.-Y. Kang, M. Lee, and T. Zyung, "Wireless energy transfer system with multiple coils via coupled magnetic resonances," *ETRI J.*, vol. 34, no. 4, pp. 527–535, Aug. 2012.

[8] B. Esteban, M. Sid-Ahmed, and N. Kar, "A comparative study of power supply architectures in wireless EV charging systems," *IEEE Trans. Power Electron.*, vol. 30, no. 11, pp. 6408–6422, Nov. 2015.

[9] P. Mercier and A. Chandrakasan, "Rapid wireless capacitor charging using a multi-tapped inductively-coupled secondary coil," *IEEE Trans. Circuits Syst.*, vol. 60, no. 9, pp. 2263–2272, Sep. 2013.

[10] Y. Lim, H. Tang, S. Lim, and J. Park, "An adaptive impedance-matching network based on a novel capacitor matrix for wireless power transfer," *IEEE Trans. Power Electron.*, vol. 29, no. 8, pp. 4403–4413, Aug. 2014.

[11] T. Beh, M. Kato, T. Imura, S. Oh, and Y. Hori, "Automated impedance matching system for robust wireless power transfer via magnetic resonance coupling," *IEEE Trans. Ind. Electron.*, vol. 60, no. 9, pp. 3689–3698, Sep. 2013.

[12] T. Imura and Y. Hori, "Maximizing air gap and efficiency of magnetic resonant coupling for wireless power transfer using equivalent circuit and Neumann formula," *IEEE Trans. Ind. Electron.*, vol. 58, no. 10, pp. 4746–4752, Oct. 2011.

[13] J. Garnica, J. Casanova, and J. Lin, "High efficiency midrange wireless power transfer system," in *Proc. IMWS-IWPT*, 2011, pp. 73–76.

[14] M. Baker and R. Sarpeshkar, "Feedback analysis and design of RF power links for low-power bionic systems," *IEEE Trans. Biomed. Ckt. Syst.*, vol. 1, no. 1, pp. 28–38, Mar. 2007.

[15] D. Ahn and S. Hong, "Wireless power transfer resonance coupling amplification by load-modulation switching controller," *IEEE Trans. Ind. Electron.*, vol. 62, no. 2, pp. 898–909, Feb. 2015.

[16] W. Zhong and S. Hui, "Maximum energy efficiency tracking for wireless power transfer systems," *IEEE Trans, Power Electron.*, vol. 30, no. 7, pp. 4025–4034, Jul. 2015.

[17] H. Li, J. Li, K. Wang, W. Chen, and X. Yang, "A maximum efficiency point tracking control scheme for wireless power transfer systems using magnetic resonance coupling," *IEEE Trans. Power Electron.*, vol. 30, no. 7, pp. 3998–4008, Jul. 2015.

[18] M. Fu, H. Yin, X. Zhu, and C. Ma, "Analysis and tracking of optimal load in wireless power transfer systems," *IEEE Trans. Power Electron.*, vol. 30, no. 7, pp. 3952–3963, Jul. 2015.

[19] T. Diekhans and R. De Doncker, "A dual-side controlled inductive power transfer system optimized for large coupling factor variations and partial load," *IEEE Trans. Power Electron.*, vol. 30, no. 11, pp. 6320–6328, Nov. 2015.

[20] X. Li, C.-Y. Tsui, and W.-H. Ki, "A 13.56 MHz wireless power transfer system with reconfigurable resonant regulating rectifier and wireless power control for implantable medical devices," *IEEE J. Solid-State Circuits*, vol. 4, no. 50, pp. 978–989, Apr. 2015.

[21] Q. Chen, S. Wong, C. Tse, and X. Ruan, "Analysis, design, and control of a transcutaneous power regulator for artificial hearts," *IEEE Trans. Biomed. Circuits Syst.*, vol. 3, no. 1, pp. 23–31, Feb. 2009.

[22] M. Kiani and M. Ghovanloo, "The circuit theory behind coupled-mode magnetic resonance-based wireless power transmission," *IEEE Trans. Circuits Syst. I, Reg. Papers*, vol. 59, no. 8, pp. 2065–2074, Sep. 2012.

[23] M. Kiani, U.-M. Jow, and M. Ghovanloo, "Design and optimization of a 3-coil inductive link for efficient wireless power transmission," *IEEE Trans. Biomed. Circuits Syst.*, vol. 5, no. 6, pp. 579–591, Dec. 2011.

[24] A. P. Sample, D. T. Meyer, and J. R. Smith, "Analysis, experimental results, and range adaptation of magnetically coupled resonators for wireless power transfer," *IEEE Trans. Ind. Electron.*, vol. 58, no. 2, pp. 544–554, Feb. 2011.

[25] D. Ahn and S. Hong, "A transmitter or a receiver consisting of two strongly coupled resonators for enhanced resonant coupling in wireless power transfer," *IEEE Trans. Ind. Electron.*, vol. 61, no. 3, pp. 1193–1203, Mar. 2014.

Dukju Ahn received the B.S. degree in electrical engineering from Seoul National University, Seoul, Korea, in 2007, and the M.S. and Ph.D. degrees in electrical engineering from Korea Advanced Institute of Science and Technology (KAIST), Daejeon, Korea, in 2010 and 2012, respectively.

He is currently with the Electronics and Telecommunications Research Institute, Daejeon, Korea, as a Senior Research Engineer. His current research interests include wireless power transfer, near-field communication, and analog/RF integrated circuit design for biomedical and portable applications.

Seongmin Kim received the B.S. and M.S. degrees from the Department of Electronic Engineering, Kyungpook National University, Daegu, Korea, in 1997 and 1999, respectively.

Since March 2001, he has been with the Electronics and Telecommunications Research Institute (ETRI), Daejeon, Korea. He has developed RF systems for WiFi, mobile wimax, LTE, LTE-A, and WPT. His current research interests include design and implementation of WPT system, control algorithm for WPT, and network management for WPT system.

Jungick Moon received the M.S and Ph.D. degrees from the Department of Electrical Engineering, Korea Advanced Institute of Science and Technology (KAIST), Daejeon, Korea, in 2000 and 2004, respectively.

He has been with the Electronics and Telecommunications Research Institute (ETRI), Daejeon, since 2004, as a Senior Member of Engineer Staff. His current research interests include developing small antenna, broadband antenna, wireless power transmission, and RF energy harvesting.

In-Kui Cho received the B.S. and M.S. degrees from the Department of Electronic Engineering, Kyungpook National University, Daegu, Korea, in 1997 and 1999, respectively, and the Ph.D. degree in electrical engineering from Korea Advanced Institute of Science and Technology (KAIST), Daejeon, Korea, in 2007.

Since May 1999, he has been with the Electronics and Telecommunications Research Institute (ETRI), Daejeon, Korea, where he has designed and developed optical backplane, optical chip-to-chip interconnect system, and magnetic resonance WPT. His current research interests include simulation and development of WPT components such as planar magnetic resonators and magnetic resonators for three-dimensional WPT.